NOTICE: The copyright law of the United States (Title 17, U.S. Code) governs the making of photocopies or other reproductions of copyrighted material. Under certain conditions specified in the law, libraries and archives are authorized to furnish a photocopy or other reproduction. One of these specified conditions is that the photocopy or reproduction is not to be "used for any purpose other than private study, scholarship, or research."

The CDC library absorbs the cost of copyright fees charged by publishers when applicable and the cost of articles and books obtained from other libraries. Copyright fees average $35.00 and fees charged by the lending libraries are between $10 and $15 per request

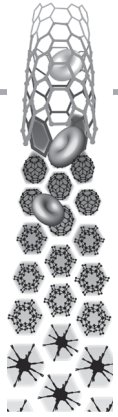

For reprint orders, please contact: reprints@futuremedicine.com

Efficient internalization and intracellular translocation of inhaled gold nanoparticles in rat alveolar macrophages

Aim: To investigate the relationship of alveolar macrophages and inhaled nanoparticles (NPs) in the lung. **Materials & methods:** Rats were exposed by inhalation to 16-nm gold NPs for 6 h, and ultramicroscopic observation on the frequency and localization of gold NPs within lavaged macrophages was performed for 7 days. **Results & discussion:** The majority of macrophages examined on day 0 (94%) contained internalized gold NPs, and the percentage decreased to 59% on day 7. Gold NPs were exclusively found within cytoplasmic vesicles. On day 0, most gold NPs appeared to be individual or slightly agglomerated, while they were frequently agglomerated on day 7. **Conclusion:** Alveolar macrophages efficiently internalized NPs by endocytosis, and rearrangements of vesicles and of NPs in the vesicles of macrophages occurred.

Original submitted 25 March 2011; Revised submitted 28 July 2011; Published online 4 April 2012

KEYWORDS: alveolar macrophage ■ cellular trafficking ■ gold ■ inhalation ■ internalization ■ nanoparticle

Shinji Takenaka*[1], Winfried Möller[1], Manuela Semmler-Behnke[1], Erwin Karg[1], Alexander Wenk[1], Otmar Schmid[1], Tobias Stoeger[1], Luise Jennen[2], Michaela Aichler[2], Axel Walch[2], Suman Pokhrel[3], Lutz Mädler[3], Oliver Eickelberg[1] & Wolfgang G Kreyling[1,4]

[1]Comprehensive Pneumology Center (CPC) – Institute of Lung Biology & Disease (iLBD), Helmholtz Zentrum München – German Research Center for Environmental Health, Ingolstaedter Landstr. 1, 85764 Neuherberg, Germany
[2]Institute of Pathology, Helmholtz Zentrum München – German Research Center for Environmental Health, Ingolstaedter Landstr. 1, 85764 Neuherberg, Germany
[3]Foundation Institute of Materials Science (IWT), Department of Production Engineering, University of Bremen, Badgasteiner Str. 3, 28359 Bremen, Germany
[4]Focus Network Nanoparticles & Health, Helmholtz Zentrum München – German Research Center for Environmental Health, Neuherberg/Munich, Germany
**Author for correspondence:*
Tel.: +49 89 3187 3097
Fax: +49 89 3187 2400
takenaka@helmholtz-muenchen.de

Because of their small size, nanoparticles (NPs; smaller than 100 nm in diameter) are considered to have specific physical and biological properties [1]. Among these, cellular internalization and intracellular redistribution are key issues associated with NPs in terms of their use in nanomedicine and possible adverse effects. The relationship between NPs and target cells has been investigated both *in vitro* and *in vivo*. Since the 1960s, *in vitro* studies by Cohn's group intensively focused on the intracellular distribution of foreign bodies, including NPs [2]. In these *in vitro* studies, administered colloidal gold NPs (Au NPs) were found in pinocytic vesicles, which accumulated at the peri- (juxta-) nuclear region of the cells [2]. Other studies using fluorescent particles, in some cases with live cell imaging, also showed peri- (juxta-) nuclear accumulation of endocytosed particles [3–6]. Moreover, the nuclear entry of modified NPs was reported recently [7–12].

The fate of inhaled NPs in the lung is more complicated compared with *in vitro* conditions. Detailed morphological studies after exposure of rodents to NPs have already been performed [13]. In these studies, NPs of iron oxide, carbon (India ink) or colloidal Au NPs introduced into the lung were found mainly in alveolar macrophages and also in the alveolar septum/connective tissue. The NPs used in these studies were applied as suspensions by intratracheal instillation (2–5 mg per mouse or neonatal rabbit) or as highly concentrated aerosols (~200 mg/m^3). All of these studies used overload conditions, which enabled the easy morphological detection of particles in the lung. In addition, the experimental conditions promoted particle agglomeration, resulting in large particle agglomerates. Such agglomerated particles, as well as particles greater than 100 nm are readily phagocytozed by alveolar macrophages [14]. On the contrary, truly nanosized particles may not be readily recognized and therefore not efficiently eliminated by alveolar macrophages in the alveolar region (initial hypothesis). A prerequisite for testing this hypothesis is that NPs should not be administered as large agglomerates, but as small nanosized particles. Our inhalation facility allows inhalation studies with an aerosol of appropriately sized NPs at relatively low concentrations [15]. Studies under these conditions, with respect to retention/clearance and systemic particle translocation, have been reported recently (Supplementary Box 1, see online at www.futuremedicine.com/doi/suppl/10.2217/NNM.11.152) [16–18]. These quantitative studies showed that low fractions of lung-retained particles were lavagable on day 1 (14–24%) and on day 7 (5–10%) after inhalation of iridium [16] or Au NPs [17]. This outcome was quite different from studies using micron-sized particles, in which approximately 80% of lung-retained iron oxide or polystyrene particles were lavagable even at 7 days after inhalation [19]. This difference supports our initial hypothesis of an

inability of alveolar macrophages to recognize NPs in the lung. Therefore, macrophages may play a minor role in NP clearance from the lung. Due to lack of morphological evidence, however, we could not determine the ultimate role of alveolar macrophages on the elimination of NPs in the alveolar region. Therefore, detailed morphological examinations using proper methods are urgently necessary.

Because of their high electron density and spherical shape ("punctate nature", according to Lucocq *et al.* [20]), 5-nm colloidal Au NPs can be easily recognized with conventional transmission electron microscopy (TEM) [20]. In the present study we analyzed macrophages in bronchoalveolar lavage (BAL) pellets of rats after a 6-h inhalation of Au NPs to elucidate the role of alveolar macrophages on the fate of inhaled NPs in the alveolar region. This morphological study addresses two major issues: the efficacy of NP endocytosis by alveolar macrophages and the intracellular particle distribution and trafficking, seeking to determine if lysosomal/nuclear trafficking occurs under these experimental conditions.

Materials & methods

Generation & characterization of Au NPs

Au NPs were generated by spark discharge under argon atmosphere (model GFG 1000, Palas, Karlsruhe, Germany). The size distribution and the number concentration were measured with a differential mobility analyzer (model EMS 150, Hauke, Gmunden, Austria) and a condensation particle counter (model 3022A, TSI, MN, USA). Mass concentration was measured by a filter sample using polytetrafluoroethylene filters (pore size 0.2 µm; Sartorius, Goettingen, Germany). The ultrastructure of Au NPs collected in the air stream from an inhalation chamber was examined by a transmission electron microscope (EM10CR, Zeiss, Oberkochen, Germany). As shown in Figure 1, the Au NPs were either individual (53% in 222 particle profiles), double (23%) or multiple (24%). Individual primary particles were spherical and electron dense, with diameters of 5–8 nm. The mean length (longest path) of triples or multiples was 27.7 ± 9.7 nm (mean ± standard deviation), and so the Au NPs were categorized as ultrafine (<100 nm). For further characterization of the Au NPs, highly concentrated aerosols of Au NPs were sampled and analyzed: they were collected on a filter for estimation of the specific particle surface area and surface charge; they were precipitated on a single crystalline Si substrate for analysis of the crystalline structure; and they were precipitated on a TEM copper grid for the elemental analysis. Specific particle surface area was assessed according to the method described by Brunauer, Emmett and Teller (BET) [21] using a PMI BET Sorptometer (Porous Materials, NY, USA). The surface charge of Au NPs in distilled water was estimated according to ζ potential measurements using a Zetasizer (Malvern Instruments, Worcestershire, UK). X-ray diffraction of Au NPs for the analysis of crystalline structure was performed using the PANalytical X'Pert MPD PRO diffracting system. The instrument was equipped with Ni-filtered Cu-K^{α} (λ = 0.154 nm) radiation, ¼° fixed divergence, primary and secondary Soller slit with 0.04 rad aperture, circular sample holder with 16 mm diameter, and X'Celerator detector (position sensitive in a range of 2.122° 2θ with 127 channels, yielding a channel width of 0.01671° 2θ), applying a continuous scan in the range of 15–140° 2θ and an integration step width of 0.0334° 2θ. The elemental analysis of NPs was obtained via energy-dispersive spectroscopy using FEI Titan™ 80-300 TEM microscope equipped with a Cs corrector for the objective lens, a Fischione high angle annular dark field detector.

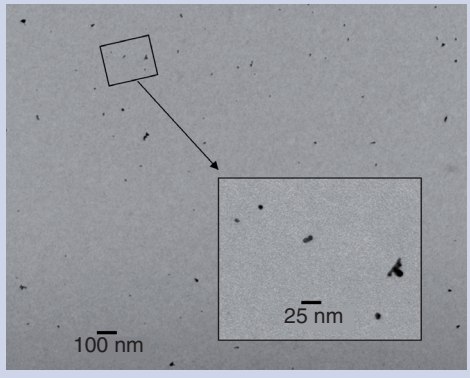

Figure 1. Ultrastructure (transmission electron microscopy) of the gold aerosol (magnification ×25,000). Inset shows enlargement of a part with higher magnification ×100,000.

Animals

Male Wistar-Kyoto rats (body weight 290–315 g on the day of exposure) were obtained from Elevage Janvier (Le Genest-Saint-Isle, France) and housed in an animal facility under filtered air conditions (24°C, 55% relative humidity). They received a standard pellet diet and water *ad libitum*. This study was conducted under German federal guidelines for the use and care

of laboratory animals and was approved by the Government of the District of Upper Bavaria and by the animal care and use committee of this research center.

Inhalation exposure & tissue preparation

Sixteen rats were exposed to Au NPs in a whole-body chamber (330 l in volume, laminar horizontal flow, ventilation exchange rate of 20 times/h) for 6 h at a mass concentration of 88 μg/m^3 and a particle number concentration of 4 × 10^6/cm^3. The inhaled Au NPs had a count median (mobility) diameter of 16 nm with a geometric standard deviation of 1.5, which is consistent with weakly agglomerated NPs of 5–8 nm primary particle size, as was confirmed by TEM analysis of a particle sample collected by diffusion from the air stream of the inhalation chamber (Figure 1).

Four rats were sacrificed at days 0, 1, 4 and 7 after exposure. Four additional rats were exposed to clean air in another whole body chamber to provide control values. Each rat was exsanguinated through collection of blood from the abdominal aorta under deep anesthesia. After separation from surrounding tissues, the weight of the whole lung was measured. The right lobes were used for the estimation of the Au concentration by means of inductive coupled plasma mass spectrometry. The left lung lobe was lavaged with 3 ml of phosphate-buffered saline (without Ca^{2+} and Mg^{2+}) three-times via the trachea after ligating the right main bronchus with an operation thread. The volume of saline used was calculated according to Kodavanti *et al.* [22] (28 ml/kg body weight for the whole lung, 9 ml/kg for the left lobe). At each time, three in-and-out washes were performed. A supplemental experiment using four rats demonstrated that this procedure yielded 0.3 ± 0.05 × 10^6/ml cells. In total, 7.2–7.7ml of lavage fluid was collected from each rat. A half milliliter of the fluid of each animal was used for the estimation of Au concentration by means of the inductive coupled plasma mass spectrometry, and the remainder of the lavage fluids was used for further morphological analysis.

The lavage fluid was centrifuged at 450 × g for 5 min after addition of 1 ml fixative (2.5% glutaraldehyde in 0.1 M potassium phosphate buffer, pH 7.4, 340 mOsm) to stop possible endocytotic activity of the macrophages [2]. The pellet for each rat was then resuspended with 0.25 ml phosphate-buffered saline. The resuspended cells of two rats were pooled, placed into embedding capsules, and recentrifuged at 450 × g for 5 min. The pellets (two pellets in each group) in the embedding capsule were further fixed with the same fixative until the embedding process. The pellets were refixed with 1% osmium tetroxide, dehydrated in a graded series of alcohols and propylene oxide, and embedded in Epon. Semithin sections were stained with toluidine blue, and BAL cell differentiation was performed for estimation of possible inflammatory reactions. Ultrathin sections (70-nm thickness) were stained with uranyl acetate and lead citrate. To minimize possible contamination, ultrathin sections of 100-nm thickness without further staining were used for examining presence of particles in the lavaged cells.

Morphological analysis

As mentioned above, Au NPs in the tissue can be ultramicroscopically recognized owing to their high electron density and round shape. We used a TEM (Zeiss EM10CR, 80 kV) fitted with a MegaView III camera and a computer-controlled digital imaging system (Olympus Soft Imaging Solution GmbH, Muenster, Germany), which enabled recording of the site of interest observed at low magnification (×2700), and later further observation at a higher magnification. With this system, cells were randomly identified as macrophages when they had typical microvilli/pseudopod characteristics and showed the whole profile of the nucleus and the cytoplasm within the square of the grid (300 mesh). For this choice, the presence of particles was not considered. The entire profile of each cell was documented by digital imaging at a magnification of ×5000.

Because labeling densities (Au NPs per profile area) can only be calculated if the lattice area per test point and specimen magnification are known [23], the total area and cytoplasm/nucleus area ratio were estimated according to the point-counting method using printed pictures (final magnification of ×7900) and the double square lattice test system B100 [24]. Since an unequivocal recognition of the cell type and structure is needed, small profiles of cells with no nucleus were not used for further analysis in this study.

Because of the small size, the precise identification of the Au NPs required a higher magnification of at least ×25000. At this magnification, the whole profile of the cells was thoroughly examined by two investigators (L Jennen and S Takenaka). At first, careful investigation was carried out regarding the presence of particles in

the cell organelles and the nucleus. The second issue for analysis was the particle localization within or outside of vesicles (free in the cytoplasmic matrix). The following issues were further analyzed:

- Agglomerated NPs: shape, size (number of individual NPs per agglomerate) and the site in the vesicle;
- NP-containing vesicles: shape, size, site within the macrophage and number of NPs according to: none, 1–9 NPs per vesicle (referred to as a 'small' number of NPs), 10–100 NPs per vesicle (middle), and greater than 100 NPs per vesicle (large).

If more than one agglomerate occurred within a vesicle, the sum of all NPs was counted and the vesicle was classified accordingly.

Statistical analysis

As mentioned above, only two cell pellets per experimental group were available for assessing the morphology of lavaged cells. In order to perform a statistical analysis regarding the time dependency of NP internalization, data from the two earlier (day 0 and 1) and the two later (day 4 and 7) time points were combined. Differences between groups were analyzed by Student's t-test. In addition, regression analysis was performed for investigating time dependency of the study parameters using the Microsoft Excel software package. Differences were considered statistically significant when $p/F < 0.05$.

Results

The present morphological study was performed following a quantitative study on retention/clearance and systemic translocation of inhaled Au NPs [17], the results of which are summarized in Supplementary Table 1. In the previous study, the Au concentration/content in the lung, the lavage fluid and the blood was estimated. The study indicated that 29 and 6% of Au NPs retained in the lung were lavagable on days 0 and 7, respectively (Supplementary Table 1). Since low fractions of polymorphonuclear leukocytes (1.2–2.4% of total BAL cells), were found in semithin sections of each pellet, the Au NPs did not show any signs of toxicity in the lung after the 6 h exposure (Supplementary Figure 1).

Characteristics of Au NPs

Physical characterization of Au NPs performed in this study includes BET (~30 m^2/g), surface charge (-24.2 mV), structure of Au by XRD (typical crystalline structure of Au) (Supplementary Figure 2), and element analysis by energy-dispersive spectroscopy (pure Au) (Supplementary Figure 3). These characteristics are consistent with pure crystalline, nonmodified Au.

As shown in Figure 1, Au NPs collected from the air stream (aerosol) showed homogeneous distribution on the TEM grid. Most particles

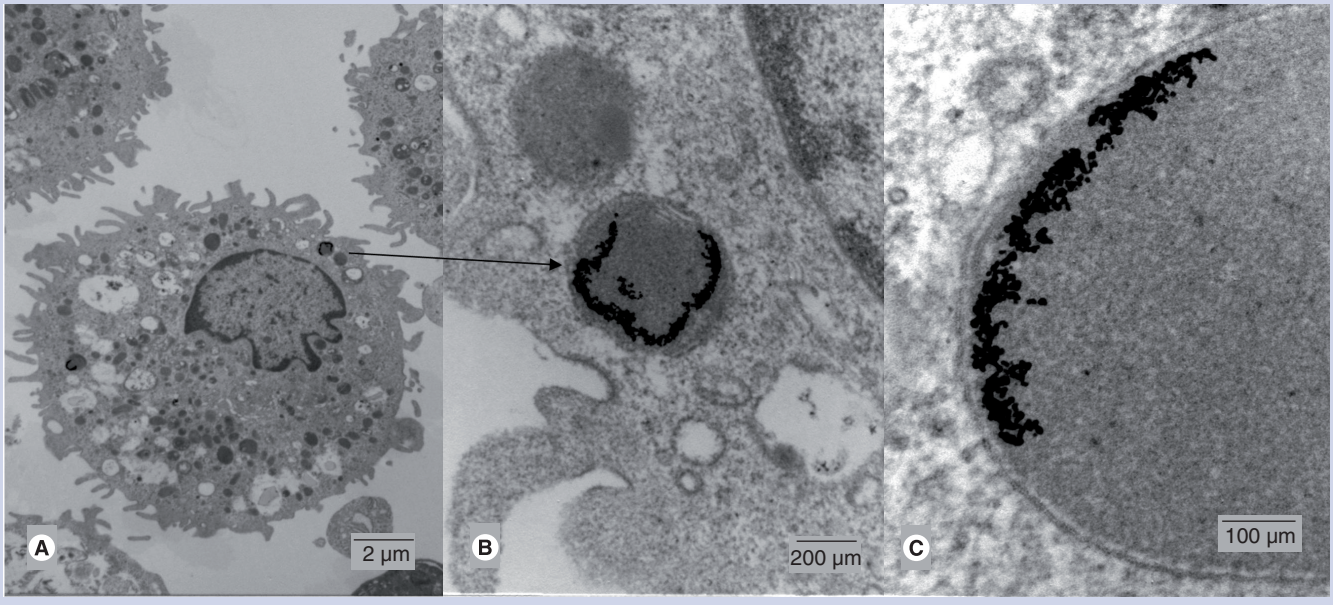

Figure 2. Lavaged macrophage on day 7. Gold nanoparticle (Au NP) agglomerates are lining up along the membrane and within the vesicle lumen. **(A)** Original magnification ×5000. **(B)** Original magnification ×50,000. **(C)** Original magnification ×120,000). Au NPs are located in close proximity to the vesicle membrane. Arrow indicates Au NP-containing vesicle in the macrophage.

were individual and few were double/triple, or low-grade agglomerates. Individual NPs were spherical with diameters of 5–8 nm both as aerosol and in the cells, even for the probes collected on day 7 (Figure 2). At a high magnification of more than ×50,000, individual particles were clearly recognizable.

Frequency of internalization of Au NPs in alveolar macrophages

The presence or absence of Au NPs in the lavaged macrophages was estimated by ultrastructural examination of the whole profile of a single section of each cell at a magnification of ×25,200. Because the profile feature is strongly dependent on the section level of a cell, the area of the cytoplasm and the nucleus was recorded. The total cell area, the mean nucleus area per cell and the nuclear area fraction (nuclear density) of each group are shown in Table 1 for each study day.

On all study days Au NPs were exclusively found within cytoplasmic vesicles of alveolar macrophages. No free Au NPs were detected either in the cytoplasm or in the nucleus. A total of 94% of the macrophages examined on day 0 contained internalized Au NPs. The number of macrophages with Au NP-containing vesicles significantly decreased with retention time from 94% on day 0 to 86% (day 1) and 68% (day 4) to 59% on day 7 (Table 1) (F = 0.0003). As shown in Figure 3, after grouping the data as described above, the difference in Au NP-containing macrophages between the early stage (days 0 and 1) and late stage data (days 4 and 7) is significant (p = 0.002).

This decrease in the number of macrophages with internalized Au NPs during the study duration of 7 days correlates with a decreasing number of vesicles per macrophage containing Au NPs, as illustrated in Figures 2, 4 & 5. As seen from Table 1 and Figure 6, the number of NP-containing vesicles per 100 µm^2 of macrophage area significantly decreased, with retention time from 13.5 to 1.7 during the 7-day observation period (p = 0.013, F = 0.0038).

Table 1. Frequency of internalization, number of gold nanoparticle-containing vesicles and size distribution of gold nanoparticle agglomerates.

Specimen	NP-laden/ examined cells (frequency, %)	NP-containing vesicles		No. of vesicles of different sized NP agglomerates† (frequency, %)			Cells examined		Nuclear density‡
		Total number§	*Per 100 µm² cell area¶*	*Small*	*Middle*	*Large*	*Total area (µm²)*	*Mean area/cell# (µm²)*	
Day 0–A	37/40 (92.5)	>547	14.6	380 (69.5)	156 (28.5)	11 (2)	3741	93.5	0.18
Day 0–B	58/61 (95.1)	>676	12.3	507 (75)	157 (23.2)	12 (1.8)	5515	90.4	0.19
Mean	(93.8)	–	13.5	(72.3)	(25.9)	(1.9)	–	92	0.19
Day 1–A	34/40 (85)	>269	7.9	199 (74)	63 (23.4)	7 (2.6)	3386	84.6	0.18
Day 1–B	78/90 (86.7)	>572	7	271 (47.4)	261 (45.6)	40 (7)	8154	90.6	0.21
Mean	(85.6)	–	7.5	(60.7)	(34.5)	(4.8)	–	87.6	0.2
Day 4–A	45/60 (75)	231	4.2	111 (48.1)	99 (42.9)	21 (9.1)	5469	91.1	0.19
Day 4–B	40/66 (60.6)	87	1.4	19 (21.8)	38 (43.7)	30 (34.5)	6294	95.4	0.19
Mean	(67.8)	–	2.8	(35)	(43.3)	(21.8)	–	93.3	0.19
Day 7–A	24/40 (60)	80	2	25 (31.3)	30 (37.5)	25 (31.3)	3974	99.4	0.18
Day 7–B	57/98 (58.2)	118	1.4	36 (30.5)	40 (33.9)	42 (35.6)	8515	87.8	0.21
Mean	(59.1)	–	1.7	(30.9)	(35.7)	(33.5)	–	93.6	0.2

On day 4, large difference between two pellets was observed in particle-containing vesicles and size (number) of gold aggregates. This time point may be the change of distribution patterns from early phase to late phase. This must be verified in a further study.
†Category of 'small', 'middle' and 'large' NP agglomerates corresponds to 1–9, 10–99 and greater than 100 gold NPs per vesicle.
‡Area of nuclei/area of cells.
§In some macrophages, an undetermined high number of NP-containing vesicles was observed. In these cases, the value recorded was 20 vesicles per cell (Supplementary Figure 2).
¶Number of NP-containing vesicles/(total area of cells examined in µm/100).
#As mentioned in 'Materials and methods', cell profiles that showed no nucleus were not registered for further examination.
A: Pellet A of pooled cells obtained from two of the four rats in a given group; B: Pellet B of pooled cells obtained from the other two of the four rats in a given group; No.: Number; NP: Nanoparticle.

Localization of internalized Au NPs in alveolar macrophages

The NP-containing vesicles were located mainly in the intermediate region of the cell, and there was no direct connection with the cell membrane or the nuclear membrane throughout the experimental period (Figures 4 & 5). This finding was also true on day 7 (Figure 2), where no tendency for an accumulation at the perinuclear region was observed.

Most Au NP-containing vesicles were round/oval in form. The size range, which varied with section level, was up to 1 µm in diameter, but mostly between 200 and 700 nm (Figure 5). The vesicles were translucent in sections without further contrast (Supplementary Figure 4), but filled with homogeneous electron-opaque granules in sections contrasted by uranyl acetate and lead citrate (Figures 5A & B). In some cases, Au NPs were found in large vesicles, which included vacuoles in their lumen (Figure 4). These vesicles are similar to 'multivesicular bodies' [25] and 'multivesicular endosomes' [26], which are considered as either late endosomes or intermediate between early and late endosomes. Additionally, we rarely found elongated vesicles containing Au NPs (Figure 4), which correspond to early endosomes [27].

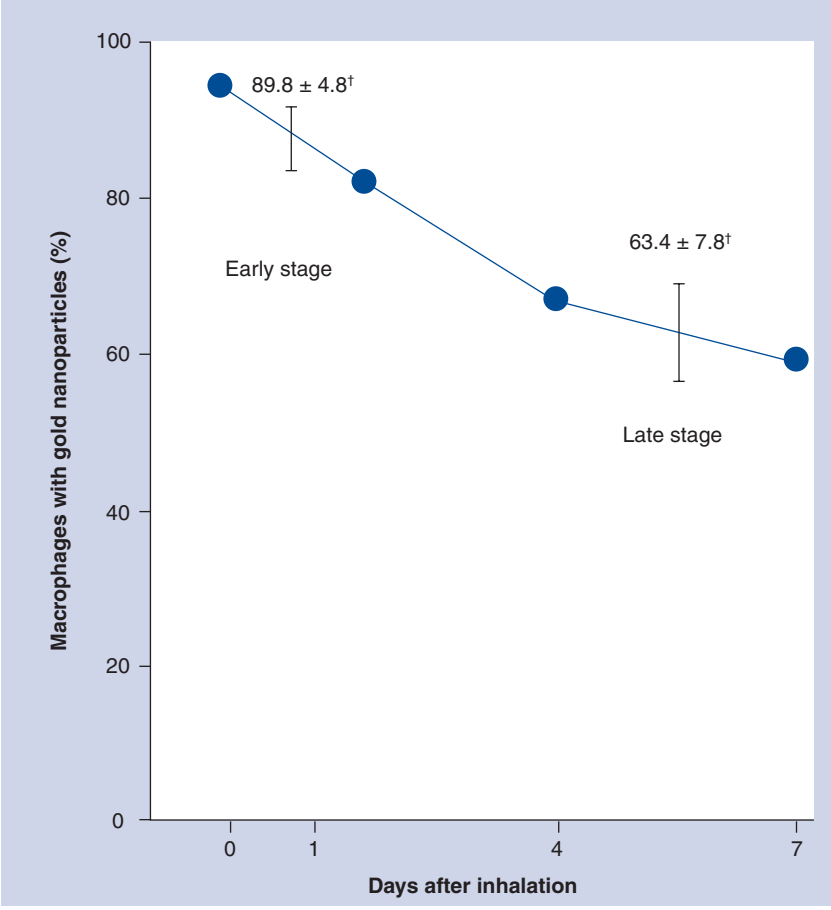

Figure 3. Percentage of macrophages with internalized gold nanoparticles.
If data from days 0 and 1 (early stage) and days 4 and 7 (late stage) are combined, respectively, the difference between both stages is statistically significant ($p = 0.002$).
†Mean ± standard deviation.

Number, site & shape of Au NPs in the vesicles

Au NPs in the vesicles were either individual, slightly agglomerated or moderately/highly agglomerated, depending on the time after Au NP inhalation. On day 0, individual or slightly agglomerated Au NPs were distributed in the vesicular lumen (Figure 4). In some cases several individual NPs were detected in one vesicle. As shown in Figure 4, individual or slightly agglomerated Au NPs could not be seen at a magnification of ×5000. However, at a magnification of ×25200, a large number of NP-containing vesicles could be detected (Figure 4; up to more than 20) and individual NPs could only be resolved at a magnification of ×50,000 or ×100,000 (Figures 4C & D). In addition to a low grade of agglomeration, few highly agglomerated particles were also found on day 0, located close to the vesicle membrane, and could be identified even at a magnification of ×5000 (Supplementary Figure 4). On days 4 and 7, most Au NPs were highly agglomerated and often located in the periphery of the vesicle, forming rod-shaped, c-shaped or ring-shaped structures (Figures 2 & 5). At a higher magnification, individual Au NPs were also identified (Figure 2). On day 1, intermediate features between those seen on day 0 and 4 were observed (Figure 5). As shown in Table 1 and Figure 7, the fraction of Au NP-containing vesicles with large numbers of Au NPs increases with time. Again, if early stage (day 0 and 1) and late stage (day 4 and 7) data are compared, a statistically significant difference was observed with respect to the fraction of small ($p = 0.008$) and large Au NP agglomerates ($p = 0.032$). Linear regression analysis showed significant time dependency, both for small agglomerates ($F = 0.011$) and for large agglomerates ($F = 0.0032$).

Discussion

Since our morphological analysis did not show any sign of toxicity in the lung tissue and in the alveolar macrophages, the internalization and redistribution/translocation processes can be considered as normal physiological processes in order to respond to NP exposure in the lung.

Our initial hypothesis, that inhaled NPs are not readily recognized and therefore not well eliminated by alveolar macrophages in the alveolar region, was in part supported by previous studies using inhaled iridium NPs and Au NPs [16,17]. This finding was mainly based on the fact that only small fractions of lung-retained particles were lavagable after NP inhalation. However, the detailed relationship between NPs and alveolar macrophages still remained to be elucidated. This morphological study revealed that alveolar macrophages engulfed inhaled Au NPs very frequently. Internalized Au NPs were found in 94% of macrophages obtained by BAL directly (day 0) after a 6-h inhalation period. The result was obtained by ultrastructural examinations of a single central section of each macrophage. Examination of the whole cell (e.g., with serial sections) would result in even higher detection rates. This high rate of internalization by alveolar macrophages was not expected, therefore, we conclude that low lavagable fractions after NP inhalation are not due to the inability of alveolar macrophages in NP recognition and endocytosis, but other issues have to be considered. The total NP burden (NP number) in the lung is one principal factor for consideration. Oberdörster *et al.* already pointed out that particles of 20 nm diameter at a mass concentration of 10 µg/m^3 represent a particle number concentration of 2.4 million particles/cm^3, whereas the same mass concentration consisting of 2.5 µm unit density particles (i.e., particles in the fine size range, PM2.5) represents only a number concentration of about 1 particle/cm^3 [28]. Thus, because of the large numbers of particles inhaled in this study (particle number concentration of 4×10^6/cm^3), the elimination of NPs from the alveolar lumen by alveolar macrophages was not complete. Even though alveolar macrophages efficiently engulf NPs in their immediate vicinity, as shown in our study, a significant number of NPs deposited far away from the macrophages may escape their endocytotic clearance function. The fate of NPs free from alveolar macrophages has been investigated [16,17,29,30], but as yet conclusive results have not been achieved [1,31]. Our quantitative study suggested that the interstitium may be the site of uptake/deposition of the NPs [30]. Further morphological studies with an appropriate design will assess the importance of the interstitium in inhaled NP retention in the lung.

The lavagable Au NP fraction at the late stage was lower than that of the early stage. At the early stage the presence of NPs outside of alveolar macrophages (free in the alveolar lumen) can not be excluded. Indeed, Semmler-Behnke *et al.* found that up to 6 h after 1 h-iridium NP inhalation, an appreciable amount of free particles was found in the BAL fluid [30]. At a later time (from 3 days), this fraction became almost undetectable. Therefore, it is plausible that the lavagable NP fraction shortly after inhalation is a mix of free and macrophage-associated NPs, and at a later time (from 4 days) no free NPs are lavagable. This may reflect the large difference in lavagable fractions between early (days 0 and 1) and late stage (days 4 and 7). The average number of internalized Au NPs per alveolar macrophage can be calculated from: the number of NPs per

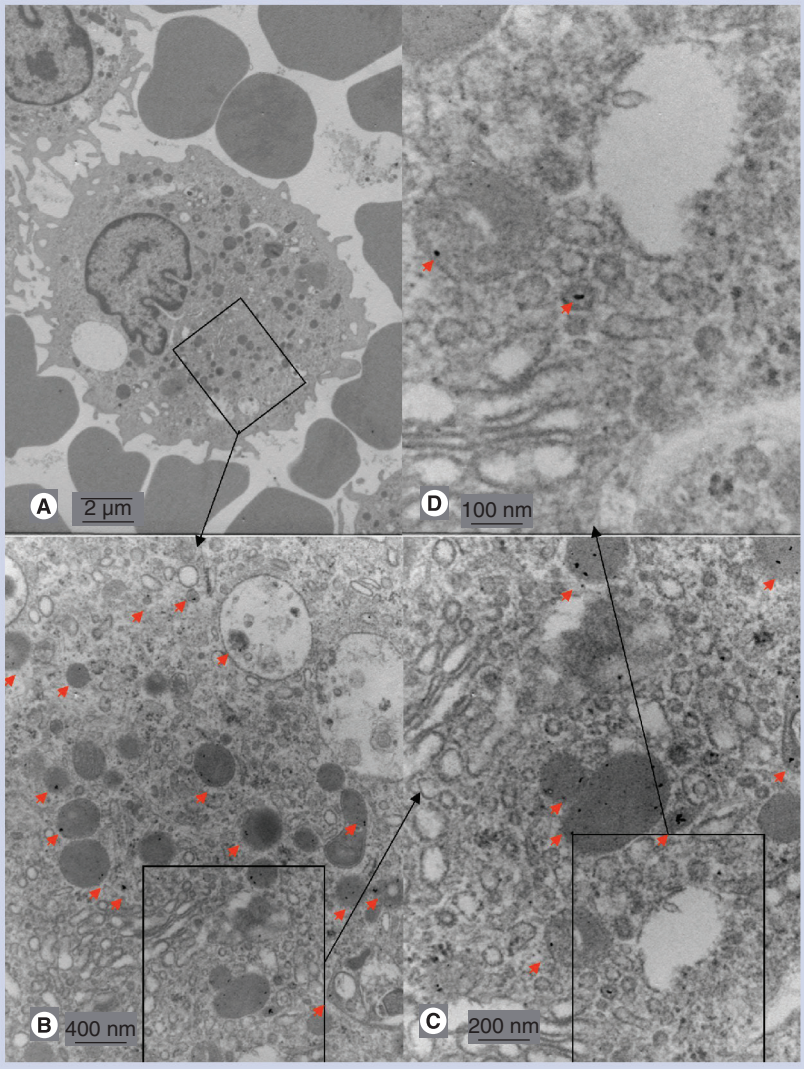

Figure 4. Lavaged macrophage on day 0 showing individual and slightly agglomerated gold nanoparticles in vesicles. (A) Original magnification ×5000. **(B)** Original magnification ×25,200. **(C)** Original magnification ×50,000. **(D)** Original magnification ×100,000. Short red arrows indicate gold nanoparticles.

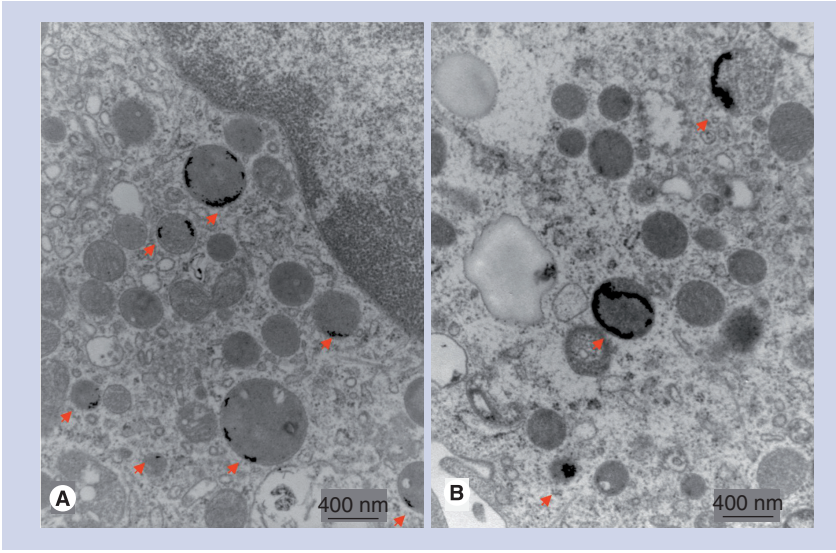

Figure 5. Agglomerates of gold nanoparticles in vesicles of a lavaged macrophage on day 1 and day 4. Gold nanoparticle (Au NP) agglomerates in vesicles of a lavaged macrophage on **(A)** day 1 and **(B)** day 4. Au NP agglomerates are located in close proximity to the vesicle membrane (original magnification ×25,200). Short red arrows indicate Au NPs.

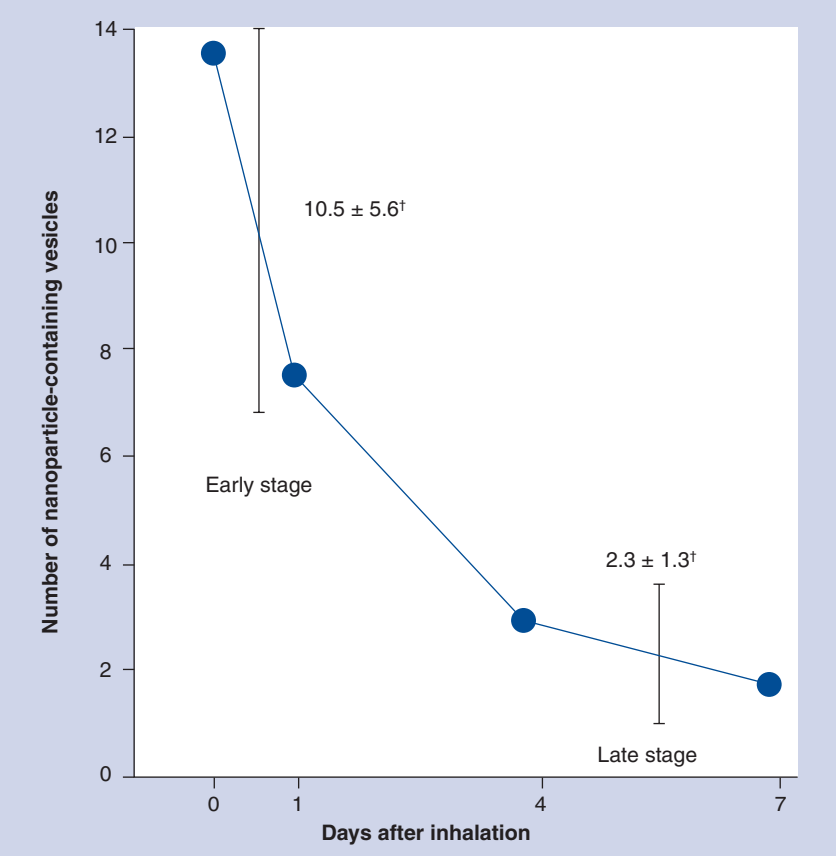

Figure 6. Number of gold nanoparticle-containing vesicles per 100 µm² of cell area examined. If data from days 0 and 1 (early stage) and days 4 and 7 (late stage) are combined, respectively, the difference between both stages is statistically significant ($p = 0.013$).
†Mean ± standard deviation.

vesicle, the number of respective NP-containing vesicles per 100 µm² cell area examined and the frequency of NP-containing alveolar macrophages. For example, the total number of Au NPs per 100 µm² cell area on day 0 would be calculated as follows: small: (13.5 vesicles per 100 µm² × 5 NPs as mean number × 0.72 as frequency) + middle: (13.5 × 50 × 0.26) + large: (13.5 × 500 × 0.019) = 49 + 176 + 128 = 353 (Table 1). According to this calculation, on average 326, 360 and 322 Au NPs internalized per macrophage are estimated for days 1, 4 and 7, respectively. This calculation suggests no significant change of the total Au NP burden per 100 µm² cell area and a prolonged retention of Au NPs within the alveolar macrophages during the experimental period of 7 days.

Au NPs were exclusively found within cytoplasmic vesicles, indicating the importance of endocytotic pathways. It has long been assumed that there are at least two pathways for endocytosis: phagocytosis (cell eating) and pinocytosis (cell drinking). Silverstein *et al.* suggested that the term 'pinocytosis' should be used to describe the uptake of all smaller substrates, ranging from insoluble particles to low-molecular weight solutes and the fluid itself, although this definition has not been used in general [32]. A recent review by Swanson also suggested that the endocytosis of particles smaller than 0.2 µm in diameter occurs through small vesicles, which form by the regulated curvature of membranes and self-assembly of ordered protein scaffolds, such as clathrin coats [33]. Contrary to other *in vitro* studies, in this *in vivo* study we did not focus on the onset of NP internalization, nevertheless, the high fraction of Au NPs found in alveolar macrophages strongly suggests active rather than passive uptake mechanisms. In this context, material-specific adsorption of proteins from the epithelial lining fluid onto the NP surface [34–36] and specific receptors, such as scavenger receptors, in alveolar macrophages [37,38] may be key factors. It was demonstrated that the scavenger receptor of macrophages is involved in NP internalization [39].

Numerous *in vitro* studies have clearly demonstrated fast intracellular trafficking (within 1 h after treatment, as a representative paper see Perera *et al.* [27]). In our long-term study (up to 7 days observation) we found that the agglomeration state of Au NPs internalized by alveolar macrophages varied as a function of time. On day 0, most of the internalized Au NPs were individual or only slightly agglomerated, and

the particles were homogeneously distributed over the vesicular lumen (Figures 4 & 6). On day 7, lower numbers of particle-containing vesicles being larger in size were found, and Au NPs were highly agglomerated (Figure 2), indicating translocation and rearrangement of the Au NPs and fusion of vesicles. The process had started even on day 0, when some highly agglomerated particles were found (Supplementary Figure 2). Agglomerates appeared as rod-shaped, c-shaped and ring-shaped structures and, as mentioned above, the agglomerates were preferentially located in close proximity to the vesicle membrane. These mechanistic issues (particle agglomeration and the preferred location of agglomerates) are not yet understood. Valberg *et al.,* using instilled colloidal Au NPs in hamsters, hypothesized that accumulation of colloidal Au NPs within a single phagolysosome may reflect the fusion of many small vesicles into one larger vesicle [40]. This kind of fusion is one possible mechanism of lysosomal biogenesis [26,41]. Hence, the enhanced state of agglomeration accompanied by fewer NP-containing vesicles per macrophage and by a reduced fraction of NP-containing macrophages can be interpreted as evidence for both intravesicular and intracellular transport of NPs.

The lavagable fraction of our Au NPs (29% on day 0, Supplementary Table 1) was only slightly greater than that of inhaled 15-nm iridium NPs (20%) [16,30]. Although both particle types had comparable count median mobility diameters (between 15 and 22 nm), most inhaled Au NPs were either individual or slightly agglomerated, while the inhaled iridium NPs were chain agglomerates consisting of a multiplicity of smaller primary particles. Because the lavagable fraction of slightly agglomerated Au NPs and highly agglomerated iridium NPs is similar, we can exclude the state of agglomeration as an influence on NP endocytosis efficiency by alveolar macrophages [16,17].

Nuclear transport of endogenous substances is essential for living cells and is tightly controlled, even though exogenous materials, such as viruses, can enter the nucleus. For therapeutic aims, modified materials have been tested as vectors for nuclear targeting [7–12]. In the present study nonmodified Au NPs were primarily located within lysosomes at an intermediate zone of the cell. In contrast to *in vitro* studies, which showed perinuclear arrangements of particle-containing vesicles [3–6], we found no Au NPs either along the nuclear membrane or within the nucleus up to 7 days. In most *in vitro* studies high particle masses were applied, resulting in much higher particle burdens per cell. Consequently, the high number of internalized agglomerates could explain the more prevalent presence of NPs in the perinuclear region in the *in vitro* studies. In addition, Au NPs, including our Au NPs, are negatively charged at even low pH [42], therefore they can only bind to elements of the lysosomal system, whereas positively charged particles can

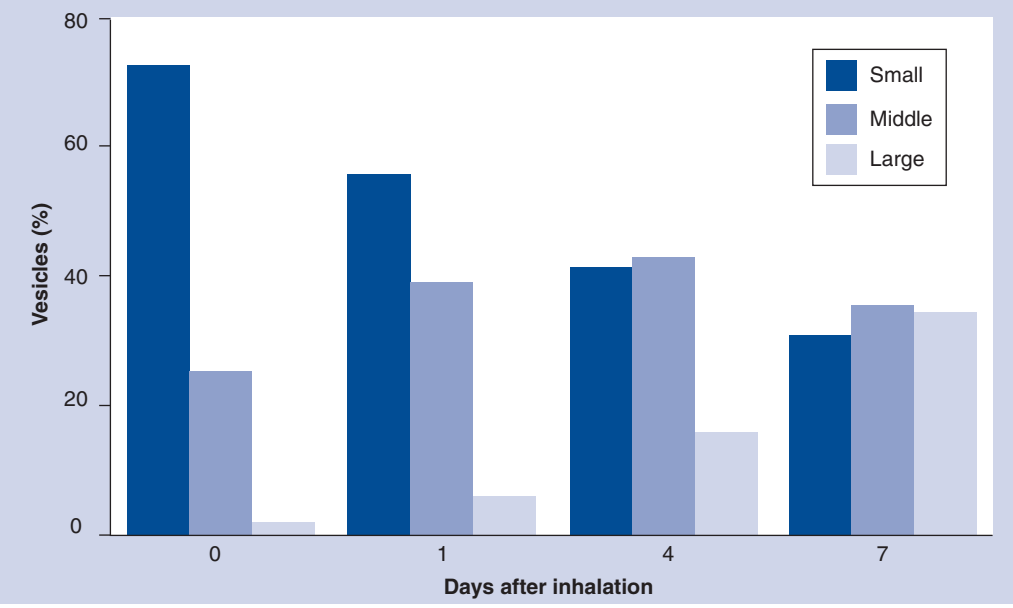

Figure 7. Fraction of gold nanoparticle-containing vesicles with small (1–9), medium (10–99) and large (>100) numbers of primary gold nanoparticles during the 7-day observation period after nanoparticle inhalation.

not only fuse with the lysosomal system, but also with elements of the secretory pathways [43,44]. This distinction may contribute to the difference in the distribution pattern of NPs within cells.

Conclusion

In contrast with our initial hypothesis, we show herein that alveolar macrophages have a high capacity to engulf even very small inhaled NPs. Internalized Au NPs are solely incorporated into lysosomal vesicles and no free Au NPs could be identified within the cytoplasm or within the nucleus. The time dependency of the number of NP-containing vesicles and in the size of NP agglomerates suggests translocation and rearrangement of both NPs and vesicles in the alveolar macrophage.

Future perspective

This study demonstrated that alveolar macrophages efficiently internalize NPs by endocytosis; therefore, they play a significant role in the elimination of inhaled NPs, which are very small but not agglomerated particles, from the alveolar lumen. Our study provided helpful information on the role of alveolar macrophages on NPs in environmental exposure and medical application.

Acknowledgements

We would like to thank X Hecht from the Technical University of Munich (Department of Technical Chemistry II, Munich, Germany) for performing the Brunauer, Emmett and Teller surface area measurements, and P Valceschini (BASF, Ludwigshafen, Germany) for the ultrastructural analysis. We also would like to thank A Rosenauer and M Schowalter, (Department of Physics, University of Bremen, Germany) for the energy dispersive technology analysis of transmission electron microscopy samples.

Financial & competing interests disclosure

The authors have no relevant affiliations or financial involvement with any organization or entity with a financial interest in or financial conflict with the subject matter or materials discussed in the manuscript. This includes employment, consultancies, honoraria, stock ownership or options, expert testimony, grants or patents received or pending, or royalties.

No writing assistance was utilized in the production of this manuscript.

Ethical conduct of research

The authors state that they have obtained appropriate institutional review board approval or have followed the principles outlined in the Declaration of Helsinki for all human or animal experimental investigations. In addition, for investigations involving human subjects, informed consent has been obtained from the participants involved.

Executive summary

- Rats were exposed by inhalation to gold nanoparticles (Au NPs), generated by a spark discharge generator for 6 h at a concentration of 88 µg/m^3 (4 × 10^6/cm^3, 16 nm mobility diameter and 5–8 nm primary particle diameter).
- Our previous Au NP inhalation study in rats showed high NP retention in the lung over 7 days and low lavagable fractions.
- This ultramicroscopic observation study on the frequency and localization of Au NPs within lavaged alveolar macrophages showed that 94% of the macrophages examined on day 0 contained internalized Au NPs, and the percentage decreased to 59% on day 7.
- Au NPs were exclusively found within cytoplasmic vesicles, which were mainly located in the intermediate zone of the cytoplasm.
- On day 0, most Au NPs appeared to be individual or slightly agglomerated. They were frequently agglomerated on days 4 and 7. Highly agglomerated particles were mostly located in the vesicle periphery, forming rod-shaped, c-shaped or ring-shaped structures.
- These findings indicate rearrangements and fusion of vesicles and of NPs in the vesicles of macrophages.
- This study demonstrates that alveolar macrophages efficiently internalize NPs by endocytosis; therefore, they play a significant role in the elimination of inhaled NPs from the alveolar lumen.

References

Papers of special note have been highlighted as:
- ▪ of interest
- ▪▪ of considerable interest

1 Oberdörster G, Oberdörster E, Oberdörster J. Nanotoxicology: an emerging discipline evolving from studies of ultrafine particles. *Environ. Health Perspect.* 113, 823–839 (2005).

▪▪ **Review of the nanotoxicological disciplines.**

2 Steinman RM, Mellman IS, Muller WA, Cohn ZA. Endocytosis and the recycling of plasma membrane. *J. Cell Biol.* 96(1), 1–27 (1983).

▪ **One paper from the many *in vitro* studies of this group on the intracellular dynamics of nanoparticles.**

3 Lai SK, Hida K, Man ST *et al.* Privileged delivery of polymer nanoparticles to the perinuclear region of live cells via a non-clathrin, non-degradative pathway. *Biomaterials* 28(18), 2876–2884 (2007).

4 Loubery S, Wilhelm C, Hurbain I, Neveu S, Louvard D, Coudrier E. Different microtubule motors move early and late endocytic compartments. *Traffic* 9(4), 492–509 (2008).

5 Luhmann T, Rimann M, Bittermann AG, Hall H. Cellular uptake and intracellular pathways of PLL-g-PEG-DNA nanoparticles. *Bioconjug. Chem.* 19(9), 1907–1916 (2008).

6 Greulich C, Diendorf J, Simon T, Eggeler G, Epple M, Koller M. Uptake and intracellular distribution of silver nanoparticles in human mesenchymal stem cells. *Acta Biomater.* 7(1), 347–354 (2011).

7 Tkachenko AG, Xie H, Liu Y *et al.* Cellular trajectories of peptide-modified gold particle complexes: comparison of nuclear localization signals and peptide transduction domains. *Bioconjug. Chem.* 15(3), 482–490 (2004).

8 Nabiev I, Mitchell S, Davies A *et al.* Nonfunctionalized nanocrystals can exploit a cell's active transport machinery delivering them to specific nuclear and cytoplasmic compartments. *Nano Lett.* 7(11), 3452–3461 (2007).

9 Berry CC, de la Fuente JM, Mullin M, Chu SW, Curtis AS. Nuclear localization of HIV-1 tat functionalized gold nanoparticles. *IEEE Trans. Nanobiosci.* 6(4), 262–269 (2007).

10 Berry CC. Intracellular delivery of nanoparticles via the HIV-1 tat peptide. *Nanomedicine (Lond).* 3(3), 357–365 (2008).

11 Nativo P, Prior IA, Brust M. Uptake and intracellular fate of surface-modified gold nanoparticles. *ACS Nano* 2(8), 1639–1644 (2008).

12 Lowe AR, Siegel JJ, Kalab P, Siu M, Weis K, Liphardt JT. Selectivity mechanism of the nuclear pore complex characterized by single cargo tracking. *Nature* 467(7315), 600–603 (2010).

13 Lauweryns JM, Baert JH. The role of the pulmonary lymphatics in the defenses of the distal lung: morphological and experimental studies of the transport mechanisms of intratracheally instillated particles. *Ann. NY Acad. Sci.* 221, 244–275 (1974).

▪▪ **An *in vivo* morphological study on the localization of nanoparticles after instillation.**

14 Oberdörster G. Lung clearance of inhaled insoluble and soluble particles. *J. Aerosol. Med.* 1(4), 289–330 (1988).

15 Roth C, Ferron GA, Karg E *et al.* Generation of ultrafine particles by spark discharging. *Aerosol. Sci. Technol.* 38(3), 228–235 (2004).

16 Kreyling WG, Semmler M, Erbe F *et al.* Translocation of ultrafine insoluble iridium particles from lung epithelium to extrapulmonary organs is size dependent but very low. *J. Toxicol. Environ. Health A.* 65(20), 1513–1530 (2002).

17 Takenaka S, Karg E, Kreyling WG *et al.* Distribution pattern of inhaled ultrafine gold particles in the rat lung. *Inhal. Toxicol.* 18(10), 733–740 (2006).

18 Takenaka S, Karg E, Roth C *et al.* Pulmonary and systemic distribution of inhaled ultrafine silver in rats. *Environ. Health Perspect.* 109(Suppl. 4), 547–551 (2001).

19 Lehnert BE, Valdez YE, Tietjen GL. Alveolar macrophage-particle relationships during lung clearance. *Am. J. Respir. Cell Mol. Biol.* 1(2), 145–154 (1989).

20 Lucocq JM, Habermann A, Watt S, Backer JM, Mayhew TM, Griffiths G. A rapid method for assessing the distribution of gold labeling on thin sections. *J. Histochem. Cytochem.* 52(8), 991–1000 (2004).

21 Brunauer S, Emmett PH, Teller E. Adsorption of gases in multimolecular layers. *J. Am. Chem. Soc.* 60, 309–319 (1938).

22 Kodavanti UP, Schladweiler MC, Ledbetter AD *et al.* Pulmonary and systemic effects of zinc-containing emission particles in three rat strains: multiple exposure scenarios. *Toxicol. Sci.* 70(1), 73–85 (2002).

23 Mayhew TM, Lucocq JM, Griffiths G. Relative labelling index a novel stereological approach to test for non-random immunogold labelling of organelles and membranes on transmission electron microscopy thin sections. *J. Microsc.* 205, 153–164 (2002).

24 Weibel ER. *Stereological methods. Volume 1. Practical Methods for Biological Morphometry.* Acadmic Press INC, London, UK (1979).

25 Katzmann DJ. No ESCRT to the melanosome: MVB sorting without ubiquitin. *Dev. Cell* 10(3), 278–280 (2006).

26 Falguieres T, Luyet PP, Gruenberg J. Molecular assemblies and membrane domains in multivesicular endosome dynamics. *Exp. Cell Res.* 315(9), 1567–1573 (2009).

27 Perera RM, Zoncu R, Johns TG *et al.* Internalization, intracellular trafficking, and biodistribution of monoclonal antibody 806: a novel anti-epidermal growth factor receptor antibody. *Neoplasia* 9(12), 1099–1110 (2007).

28 Oberdörster G, Gelein RM, Ferin J, Weiss B. Association of particulate air pollution and acute mortality: involvement of ultrafine particles? *Inhal. Toxicol.* 7(1), 111–124 (1995).

29 Furuyama A, Kanno S, Kobayashi T, Hirano S. Extrapulmonary translocation of intratracheally instilled fine and ultrafine particles via direct and alveolar macrophage-associated routes. *Arch. Toxicol.* 83(5), 429–437 (2009).

30 Semmler-Behnke M, Takenaka S, Fertsch S *et al.* Efficient elimination of inhaled nanoparticles from the alveolar region: evidence for interstitial uptake and subsequent reentrainment onto airways epithelium. *Environ. Health Perspect.* 115(5), 728–733 (2007).

31 Mühlfeld C, Rothen-Rutishauser B, Blank F, Vanhecke D, Ochs M, Gehr P. Interactions of nanoparticles with pulmonary structures and cellular responses. *Am. J. Physiol. Lung Cell Mol. Physiol.* 295(5), L817–L829 (2008).

32 Silverstein SC, Steinman RM, Cohn ZA. Endocytosis. *Ann. Rev. Biochem.* 46, 669–722 (1977).

33 Swanson JA. Shaping cups into phagosomes and macropinosomes. *Nat. Rev. Mol. Cell Biol.* 9(8), 639–649 (2008).

34 Chithrani BD, Ghazani AA, Chan WC. Determining the size and shape dependence of gold nanoparticle uptake into mammalian cells. *Nano Lett.* 6(4), 662–668 (2006).

35 Lundqvist M, Stigler J, Elia G, Lynch I, Cedervall T, Dawson KA. Nanoparticle size and surface properties determine the protein corona with possible implications for biological impacts. *Proc. Natl Acad. Sci. USA* 105(38), 14265–14270 (2008).

36 Lesniaka A, Campbell A, Monopoli MP, Lynch I, Salvati A, Dawson KA. Serum heat inactivation affects protein corona composition and nanoparticle uptake. *Biomaterials* 31(36), 9511–9518 (2011).

37 Palecanda A, Paulauskis J, Al-Mutairi E *et al.* Role of the scavenger receptor MARCO in alveolar macrophage binding of unopsonized environmental particles. *J. Exp. Med.* 189(9), 1497–1506 (1999).

38 Kobzik L, Godleski JJ, Brain JD. Selective down-regulation of alveolar macrophage oxidative response to opsonin-independent phagocytosis. *J. Immunol.* 144(11), 4312–4319 (1990).

39 Kanno S, Furuyama A, Hirano S. A murine scavenger receptor MARCO recognizes polystyrene nanoparticles. *Toxicol. Sci.* (2007).

40 Valberg PA, Brain JD, Kane D. Effects of colchicine or cytochalasin B on pulmonary macrophage endocytosis *in vivo*. *J. Appl. Physiol.* 50(3), 621–629 (1981).

41 Van Meel E, Klumperman J. Imaging and imagination: understanding the endo-lysosomal system. *Histochem. Cell Biol.* 129(3), 253–266 (2008).

42 Dougherty GM, Rose KA, Tok JBH *et al.* The zeta potential of surface-functionalized metallic nanorod particles in aqueous solution. *Electrophoresis* 29(5), 1131–1139 (2008).

43 Farquhar MG. Recovery of surface membrane in anterior pituitary cells. Variations in traffic detected with anionic and cationic ferritin. *J. Cell Biol.* 77(3), R35–R42 (1978).

44 Patil ML, Zhang M, Betigeri S, Taratula O, He H, Minko T. Surface-modified and internally cationic polyamidoamine dendrimers for efficient siRNA delivery. *Bioconjug. Chem.* 19(7), 1396–1403 (2008).

Reproduced with permission of the copyright owner. Further reproduction prohibited without permission.